Aerodynamic and Structural Studies of Joined-Wing Aircraft

Ilan Kroo* and John Gallman†
Stanford University, Stanford, California 94305
and
Stephen Smith‡
NASA Ames Research Center, Moffett Field, California 94035

A method for rapidly evaluating the structural and aerodynamic characteristics of joined-wing aircraft was developed and used to study the fundamental advantages attributed to this concept. The technique involves a rapid turnaround aerodynamic analysis method for computing minimum trimmed drag combined with a simple structural optimization. A variety of joined-wing designs are compared on the basis of trimmed drag, structural weight, and, finally, trimmed drag with fixed structural weight. The range of joined-wing design parameters resulting in best cruise performance is identified. Structural weight savings and net drag reductions are predicted for certain joined-wing configurations compared with conventional cantilever-wing configurations.

Nomenclature

$A_1, A_2, A_{\text{total}}$	= structural material areas (Fig. 3)
$A\!R$	= aspect ratio
b	= span
C_d	= section drag coefficient
C_D	= aircraft drag coefficient based on reference area
$C_{d0}, C_{d1}, C_{d2},$	= section viscous drag coefficients
C_ℓ	= section lift coefficient
C_L	= aircraft lift coefficient based on reference area
c	= local chord length
c_{ref}	= reference chord, $= S_{\text{ref}}/b$
M	= bending moment in local coordinates
S_{ref}	= reference area (wing plus tail area)
sm	= static margin (in reference chords)
StrBoxC	= ratio of structural box chord to airfoil chord
T_{box}	= local structural box thickness (Fig. 3)
t/c	= thickness to chord ratio
X_{tail}	= distance from c.g. to tail root quarter chord

Subscripts

p	= viscous drag component
ref	= reference value
t	= tail
w	= wing
x, y, z	= component in respective coordinate direction

*Assistant Professor, Department of Aeronautics and Astronautics. Member AIAA.
†Graduate Student, Department of Aeronautics and Astronautics. Member AIAA.
‡Aerospace Engineer, Advanced Aerodynamic Concepts Branch. Member AIAA.

Introduction

THE joined wing is an unconventional aircraft configuration with a structural connection between the main wing and horizontal tail, as shown in Fig. 1. Weight savings and aerodynamic advantages associated with this nonplanar geometry have been predicted in several studies.[1,2] In 1984, a research program was initiated at NASA Ames Research Center to quantify the gains that might be expected from such a configuration. Although several additional advantages have been suggested (including direct lift and sideforce control), the present study deals only with potential improvements in cruise efficiency. Aerodynamic analyses have suggested drag savings for configurations with large-span aft wings,[3] whereas structural sizing studies[4,5] predicted rather substantial reduc-

Baseline Joined Wing

Weight = 100,000 lb
Area = 1268.0 ft
b_W = 93.3 ft
b_t/b_W = 0.6
Wing Dihedral = 5.0
Wing Sweep = 30
Wing Taper = 0.25
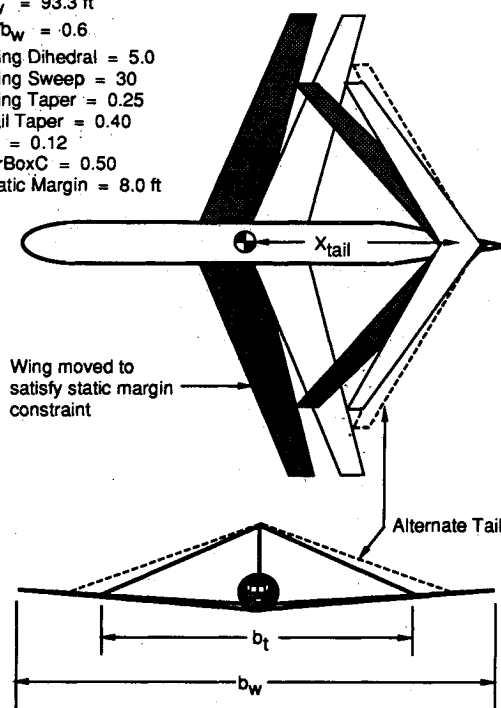Tail Taper = 0.40
t/c = 0.12
StrBoxC = 0.50
Static Margin = 8.0 ft

X_{tail}

Wing moved to satisfy static margin constraint

Alternate Tail

b_t

b_w

Fig. 1 Joined-wing configuration.

tions in structural weight for designs with inboard joint locations. Maximum performance improvements are only obtained with an appropriate compromise between potential aerodynamic and structural benefits. Results from the current study suggest that the structural efficiency of the joined-wing concept is its primary advantage. The most promising joined-wing designs (from the standpoint of cruise efficiency) utilize inboard wing joints and use the concept's structural advantage to increase wing span and reduce induced drag.

The goal of this investigation was to provide tools for use in the early stages of joined-wing aircraft design definition and to quantify some of the savings that might be expected from such a design. The results are intended to provide a clear picture of the fundamental advantages and disadvantages of the design concept. A complete design comparison would involve the design synthesis of a complete aircraft and is beyond the scope of the current paper. Nevertheless, the basic results obtained here suggest that there is reason to consider this configuration for certain applications; they provide a starting point for more detailed application studies, some of which are currently underway.

Basic Approach

To assist in tradeoffs at the preliminary design level, a rapid turnaround analysis and design program was developed. The method combines an optimizing vortex-lattice aerodynamics code with a fully stressed beam sizing routine to estimate potential savings in trimmed drag, structural weight, or trimmed drag with a fixed structural weight.
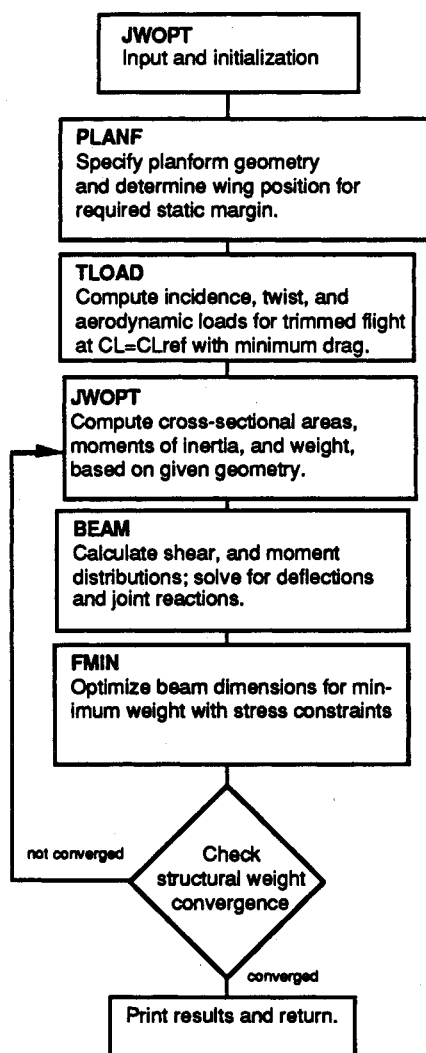

Fig. 2 Outline of analysis method.

Several basic assumptions are required to generate comparable results for conventional and joined-wing configurations. The most significant simplifying assumption in this analysis is the restriction to a single cruise design point. Critical structural loading may occur at several different flight conditions, but for the purposes of this comparison, the structural loading was determined by multiplying the trimmed lift distributions at cruise by a typical load factor. All comparisons are done at a given airspeed and altitude. A second iteration would allow designs with lower induced drag to better utilize this advantage by flying higher, but correct trends appear in the fixed-C_L data.

The other major assumption is that the aircraft total lifting surface area is constant. A more rational constraint might include field length requirements so that aircraft with higher $C_{L_{max}}$ values could utilize smaller wings with lower parasite drag. The computation of landing field length and $C_{L_{max}}$ introduces variables that truly require a complete aircraft synthesis study, greatly complicating and specializing the analysis. Thus, the results here apply only to cruise performance with fixed area. If the joined-wing design of interest is capable of achieving higher $C_{L_{max}}$ values than a conventional aircraft, the resulting cruise drag after resizing will be reduced. A penalty in $C_{L_{max}}$ will result in higher cruise drag of the resized aircraft, and this possibility must be recalled when examining the results presented here. This situation seems quite possible in certain cases for which the optimum joined wing has a very small tail arm. The selection of a fixed wing + tail area also reduces uncertainties associated with the part of wing weight not associated with structural loads. In this study, the gross weight of the aircraft is assumed fixed. Thus, it is not necessary to estimate the actual wing weight— only to consider the changes in weight with different loadings and spans. Similarly, the weight and drag of the fuselage, nacelles, pylons, and vertical tail are not relevant for this analysis. It is simply the weight and drag of the lifting system that are compared in relative terms.

With these goals and assumptions, the initial approach involved varying selected joined-wing design parameters and studying the effect on drag and structural weight with a fixed wing span. Of course, a structural weight advantage can be translated into an induced drag advantage by increasing the span, and the final aspect of this study involved changing the span of the joined wing so that drag comparisons could be made at a fixed structural weight. Subsequent iterations would amplify the trends shown here as changes in required fuel weight lead to changes in cruise drag. The computer program developed for these studies consists of an integrated aerodynamic and structural design method, summarized in Fig. 2.

Aerodynamic Optimization

Geometric Constraints

The large number of variables required to specify the joined-wing geometry makes a comprehensive comparison of a wide range of joined-wing geometries difficult. The problem is made more tractable by careful selection of geometric constraints. These constraints are used to fix certain less important design parameters and link other variables to assure geometric compatibility. Selected values for the baseline joined-wing configuration are shown in Fig. 1. The first constraint imposed here involves the wing sweep. Although the optimal wing sweep may be computed after a detailed study of the effects of sweep and section thickness on compressibility drag, structural weight, and stalling characteristics, a range of reasonable wing sweeps for transport aircraft is well established. Thus, a fixed value of wing sweep was adopted for all designs.

The second geometric constraint involves the placement of the horizontal tail root at the top of the vertical tail. In this study, the vertical tail span is specified, therefore, the vertical

separation of the wing and horizontal tail is fixed. The horizontal tail sweep could be taken as a design variable that, together with the wing sweep, would determine the wing position. However, transport aircraft are the focus of the present investigation, and, for these designs, the fuselage geometry dictates the distance from the tail to the center of gravity (c.g.). Thus, the procedure used here involves specifying the longitudinal distance from the c.g. to the tail root chord and varying the wing position to obtain a joined wing with a specified static margin. The sweep and dihedral of the tail are adjusted so that its tip meets the wing.

The wing location is determined by making an initial estimate of its position, determining the static margin, and repositioning the wing. The iteration continues until the desired static margin is achieved. The required static margin depends, to some extent, on the arrangement of lifting surfaces, especially as this affects the aircraft damping. But it is perhaps more strongly influenced by the fuselage, engine, and payload arrangement as these determine the c.g. range and moment of inertia in pitch. Thus, for this study, the dimensional distance from c.g. to neutral point is held constant; that is, sm is normalized by a constant reference chord, rather than the wing mean aerodynamic chord, which changes with tail area and wing span. The selected static margin results in a 3% tail download to trim the conventional reference geometry, a value typical of existing transport aircraft.

In summary, the analysis uses the following geometric parameters to describe the configuration: wing sweep, taper, dihedral, and thickness to chord ratio; tail taper and thickness to chord ratio; distance from c.g. to tail root X_{tail}; span ratio b_t/b_w; relative aspect ratio $A\!R_t/A\!R_w$; and required static margin sm. The effects of changes in wing taper ratio, X_{tail}, b_t/b_w, $A\!R_t/A\!R_w$, and sm are discussed in this paper. The design optimization, described in more detail in the following sections, involves computation of wing position, wing and tail incidence and twist, and structural material thicknesses for minimum drag and structural weight.

Aerodynamic Analysis

The aerodynamic analysis routine must compute the static margin of the nonplanar, multiple surface arrangement for use in the planform definition phase of the program. It must also compute the loads on each of the surfaces for use in the structural calculations and the drag of the interfering surfaces for performance comparisons. The basic computational procedure uses a version of the LinAir program[6] to determine the load distributions and drag of the lifting system. The program is a form of a vortex-lattice method with a Trefftz-plane induced drag calculation and a parabolic profile drag approximation. Lift-dependent section drag is specified in the form: $C_{d_p} = C_{d_0} + C_{d_1}C_\ell + C_{d_2}C_\ell^2$ and integrated over the span of each surface. Inclusion of these terms in the optimization prevents large excursions of section C_ℓ on highly tapered wings. The value used for C_{d_0} affects the drag comparisons by changing the relative importance of induced drag penalties or advantages: the relative improvement in total drag would be reduced if C_{d_0} were increased. The absolute magnitude of performance differences among the configurations would be correct only if the fuselage and other drag contributions were added. Therefore, the present study produces only relative comparisons of the designs. For typical transport aircraft, the lifting surface drag accounts for approximately 65% of the total cruise drag.

A method for computing surface incidence and twist resulting in minimum trimmed drag was developed for use with the LinAir routine. Lifting surfaces are assumed to be twisted linearly from root to tip and are modeled with a single bound vortex line located at the section quarter-chord point. A section pitching moment coefficient is specified, and the resulting trimmed loads are incorporated in the structural analysis. It should be noted that the lift distribution for minimum drag with fixed span is not the same as that for minimum drag with

fixed weight, but the differences have been shown to be quite small[7] and would not be expected to alter the conclusions of this study. The LinAir subroutine is called five times with different root and tip incidences on each surface. This produces the linear influence coefficients required to express the total lift, drag, and moment. The total lift and the trim constraint, including the effect of section camber, are appended with Lagrange multipliers to the linear system of equations expressing the condition for minimum drag. The solution of this system provides trimmed drag and the trimmed cruise load distribution on each of the surfaces.

Structural Optimization

After the basic geometry and load distributions in cruise have been determined from the design variables and aerodynamic constraints, the structural analysis and design is performed. The simplified design loading condition is the trimmed cruise load (lift and drag), increased by a constant design load factor and modified by inertial relief effects.

The required material thicknesses for joined-wing structures, unlike those for conventional cantilever wings, depend on the stiffness of the structure. (The system is redundant.) The stiffness depends, in turn, on the required material thickness so that the problem must be solved iteratively. Thus, the iteration begins with an initial estimate of average structural box thickness. With these loads and box properties, the deflections and rotations of each surface in the three axes directions are computed. New material thicknesses within the structural box are found by satisfying a maximum stress constraint, and the iteration is repeated until the process converges.

Structural Box Model

Two structural box models were used in these studies. Initially, a symmetrical box with caps and webs of uniform thickness was used. This model is shown on the left side of Fig. 3. The skin thicknesses were represented by two design variables for each spanwise element. In this structural box model, the rectangular box occupies the full thickness of the wing. A more realistic model might include skin curvature, with reduced box depth at forward and aft webs, but this simplified model introduces little error in the bending inertia of the box, because the majority of the cap material is separated by the full wing thickness.

Previous studies[1,4,5] have indicated that the most desirable structural arrangement for joined-wing spars is asymmetric, with most of the material concentrated in opposite corners of the structural box. To evaluate the effect of the asymmetric spars on aircraft weight and drag, a more complex, asymmetric structural box model, shown on the right side of Fig. 3, was used. The two design variables are the cross-sectional areas of the stringers, A_1 and A_2 (diagonally opposite stringers have the same area). The web and cap thicknesses add two more design variables, but these are decoupled since the skins are assumed to carry shear and torsion loads only. Since the material that resists bending is now concentrated in the corners of the box (see Fig. 3), the assumption that the structural box maintains the full wing thickness was also removed. The depth of the asymmetric structural box was reduced as a function of spar width so that the box would fit into a slightly supercritical airfoil section. This produces a weight penalty for conventional cantilevered wing structures where the primary bending moments are in the chordwise direction. Thus, sections of the wing outboard of the joint (and the conventional reference design) use structural boxes that extend over just the thickest 20% of the section.

Structural Analysis

The structural box is represented by a simple beam with equivalent cross-sectional area and inertia tensor. A matrix of influence coefficients is constructed, describing the effect of unit joint-reaction forces and moments on joint rotations and
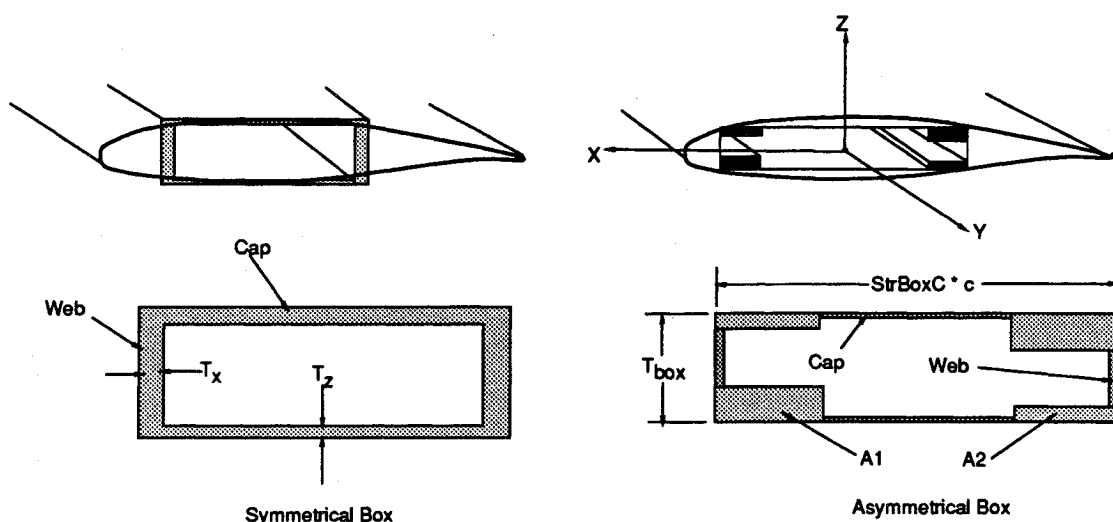
Fig. 3 Structural box geometry.

deflections. The joint reactions required to force the aft surface tip to meet the wing at the desired joint location, with the existing aerodynamic loading, are then computed. Both wings are cantilevered at the root and the joint is assumed rigid so that no relative rotation between wing and tail is permitted in any direction. This constraint is easily relaxed, although results from Ref. 8 suggest that the rigid joint is probably the best choice. Once the joint reactions have been determined, the stresses in the structural box are computed and the material thicknesses at each spanwise station can be resized.

Although this analysis neglects shear lag effects and is less detailed than previous finite element models,[9] the results of these earlier studies suggest that such effects are not of great importance for the high aspect ratio, bending-dominated structures of interest here. Results from this linear model compare very well with nonlinear finite element results until the deflections become very large or buckling of the aft surface occurs.

Optimum Material Sizing

The method used to determine the optimal material distribution within the structural box is different for the two structural box models, but, in both cases, the objective is to minimize the total weight by minimizing the cross-sectional area of each spar element, subject to maximum stress and minimum gauge thickness constraints. The wing spar is divided into 20 spanwise elements. The tail spar is divided into corresponding elements of the same span fraction, so that the number of spar elements in the tail depends on the span-ratio of the two wings.

Symmetrical Box

The cap and web thickness at each station must be sized to keep the maximum stress below a selected value. A unique feature of joined-wing structure is that the joint reactions give rise to bending moments that are not found in conventional cantilevered wings. The resultant bending moment is not aligned with the principal axis of the spar, and the maximum stress occurs at one of the four corners of the box. The distribution of material that results in a maximum stress equal to the design stress level must be determined. This is not as straighforward as it appears, as more than one solution exists. The two design variables, cap and web thickness, are linked by the maximum stress constraint; therefore, a one-dimensional search method was used to find the minimum weight solution. After the cap and web thicknesses have been computed, the structure is reanalyzed using new stiffness and mass properties. The process continues until convergence is ob-

tained. For these cases, convergence to approximately 0.1% was demanded, requiring 5–10 iterations.

Asymmetrical Box

The stringers in the corners of the box are sized to keep the stress in the structure at or below the the design stress level. Shifting material from the understressed corner of the box toward the higher stressed corner leads to an asymmetric spar geometry with less total material. The optimum degree of asymmetry occurs when the stress in adjacent corners is equal. The maximum stress constraint applied to the two adjacent corners then reduces to an expression of an optimum cross-sectional area and the optimum degree of asymmetry, eliminating the need for the nonlinear search.

An effective minimum gauge constraint is imposed by ensuring that the cross-sectional area of the four stringers is at least as great as a uniform box of minimum gauge thickness. Finally, the shear panels are sized directly to carry the shear stresses. After the stringer areas and skin thicknesses have been computed, the structure is reanalyzed.

Results

This aerodynamic and structural optimization was used to study the effects of several design variables on the relative
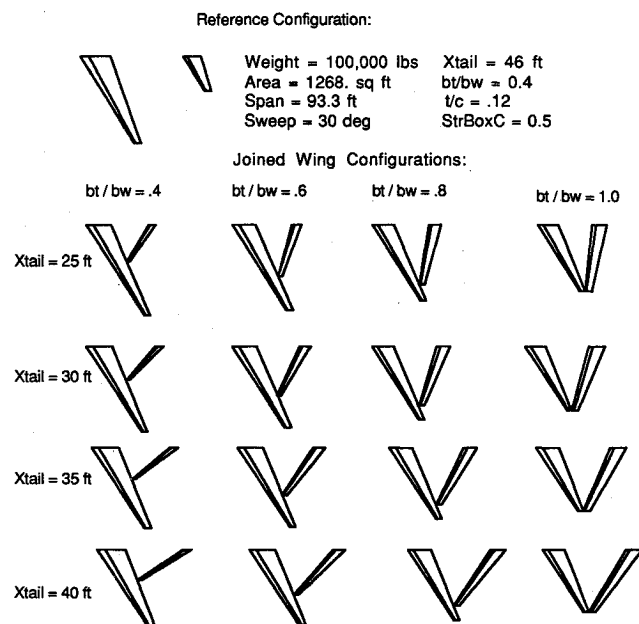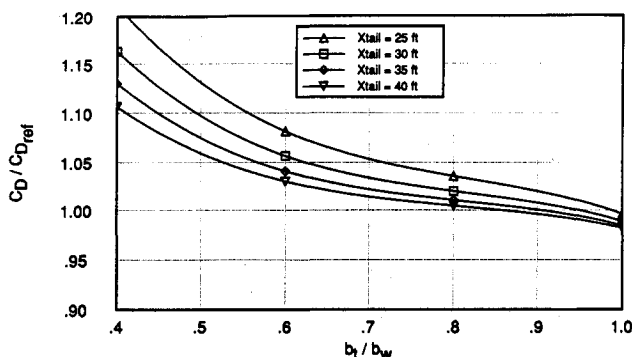

Fig. 4 Candidate joined-wing designs.

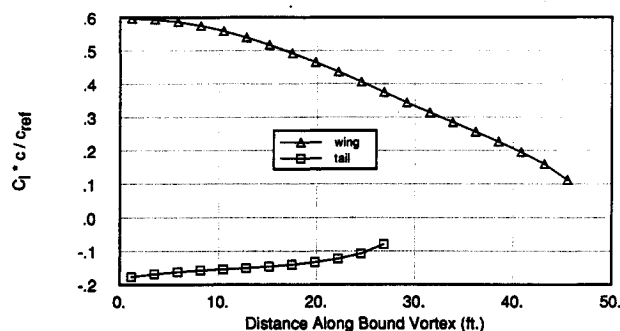**Fig. 5   Relative drag vs span ratio and tail length (fixed span).**

Fig. 6   Wing and tail lift distributions (typical joined-wing case).

weight and trimmed drag of joined-wing configurations. The results are normalized by the weight and drag of the conventional reference case, a typical medium-range transport aircraft with T-tail and aft-mounted engines. Key dimensions of the reference case are shown in Fig. 4. The wing-tail system of this reference airplane was analyzed using the same code as the joined-wing cases to provide valid comparisons. Results are presented for the range of joined-wing span ratios b_t/b_w and tail lengths X_{tail}, shown in Fig. 4. Comparisons of aerodynamics and structures are made first with fixed wing span and then with fixed structural weight. The fixed weight comparisons were done by varying the span of the forward surface in an outer iteration loop until the weight of the optimized structural boxes converged to the fixed reference value.

Trimmed Drag—Fixed Span

Drag of the joined-wing lifting systems, normalized by the drag of the conventional design with the same span, is shown in Fig. 5. It is apparent that the configurations with the largest tail lengths and tail spans achieve the lowest drag, but even these designs do not produce significant drag savings in comparison with the reference case. This conclusion appears to conflict with that of Ref. 3 in which induced drag savings of order 10–20% were achieved. The apparent contradiction is resolved by noting that induced drag reductions are only possible when the aft surface carries a significant upload, and for the selected static margin and tail lengths used in this study, the aft surface carries little lift or a moderate download. This is a result of the large static margin and the unusually small distance between wing and tail aerodynamic centers. If the distance from aircraft c.g. to tail root is fixed, most joined-wing designs have smaller tail arms due to the forward sweep of the aft surface, and the tails carry more download than a conventional tail of similar size. As can be seen from the figure, shorter tail lengths and smaller tail spans produce large drag penalties for these joined wings, and the tip-joined designs are apparently most desirable. This conclusion is substantially changed when structural weight is considered, as discussed in the next section. The computed trimmed

lift distribution for an example joined-wing design ($b_t/b_w = 0.6$, $X_{tail} = 30$ ft) is shown in Fig. 6. The large tail download is evident and the tail carries little lift near its tip. This result is expected in light of the linear wing twist distribution assumed for this study. More complex twist distributions could be used to reduce the required tail loads and the associated trim drag penalty.

Structural Weight—Fixed Span

The resulting bending moments and optimal distribution of structural material (using the symmetric box model) for this example joined-wing case are shown in Figs. 7–9. The distribution of out-of-plane bending moment M_x is shown in Fig. 7. The wing, outboard of the joint, acts as a conventional cantilever wing with a monotonically increasing bending moment from tip to joint. Whereas the moment applied to a conventional design would continue to increase from tip to root, the joined-wing bending moment is relieved by the joint reaction, falling to nearly zero at one point, and then increasing to a root moment just higher than that at the joint. The tail moments are small despite the unusually high download, but the tail carries a large compressive load that produces the joint reaction responsible for the low root bending moment in the wing. Because the tail is swept forward, the tail pushes the wing forward as well as down, resulting in a linearly varying in-plane moment M_z, shown in Fig. 8. In this case, the value of M_z at the root is many times larger than M_x. As a result, the weight of the wing web material is considerable, especially near the root, as shown in Fig. 9, which shows the distribution of weight throughout the joined-wing structure. The weight of the tail caps are greater than the webs, reflecting the bending moment imposed by the tail download. The tail thicknesses vary less than those of the wing structural box, partly because much of the tail load is a constant axial compression. The cap and web are sized to withstand the stress of the combined loading, but no consideration was made of weight penalties associated with preventing buckling. This possibility remains an important consideration for joined wings and should be addressed in future investigations.
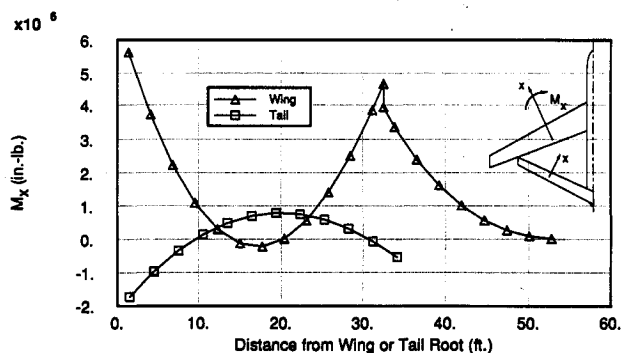

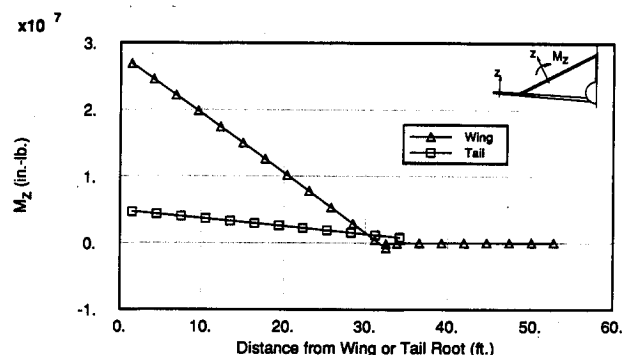**Fig. 7   Moment distribution M_x (typical joined wing).**

Fig. 8   Moment distribution M_z (typical joined wing).

Figure 10 illustrates the optimal distribution of material in the asymmetric spar box mode. The ratio A_1/A_{total} represents the amount of material required in the lower leading-edge and upper trailing-edge areas compared with the total (see Fig. 3). Values of 0.5 imply a symmetric distribution. The concentration of material in the upper leading-edge area near the wing root is caused by the combined positive values of M_x and M_z in this region. The distribution over the remaining part of the wing and tail is configuration dependent.

The result of varying the parameters X_{tail} and b_t/b_w for the symmetrical-spar joined wings is demonstrated in Fig. 11. The conclusions are just opposite to those obtained from the aerodynamic analysis: short tail arms and smaller tail spans are preferred from a structural viewpoint. The reasons for this are clear: Shorter tail arms reduce the tail sweep and permit the tail to relieve out-of-plane bending moments without introducing large M_z moments. Large span tails are penalized for several reasons. One of the most important is that with a fixed ratio of tail aspect ratio to wing aspect ratio, larger span ratios imply a more equal division of area between the two surfaces. This leads to a smaller wing chord and reduced structural box dimensions (thickness and chord). The tip-joined configurations appear terrible in this respect, with weight penalties of order 50%. The inboard joint designs, by
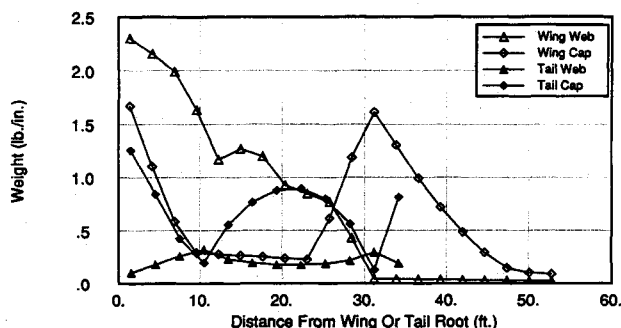
Fig. 9 Weight distribution in structural box (typical joined wing).
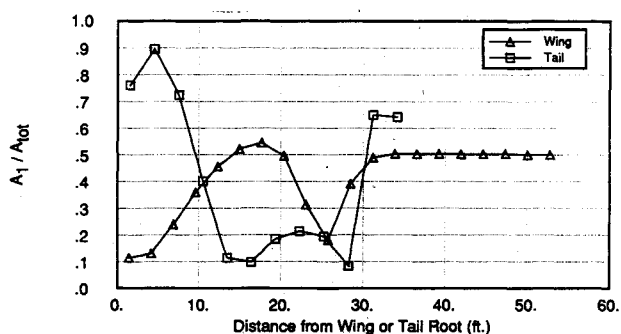
Fig. 10 Distribution of material in asymmetric structural box.
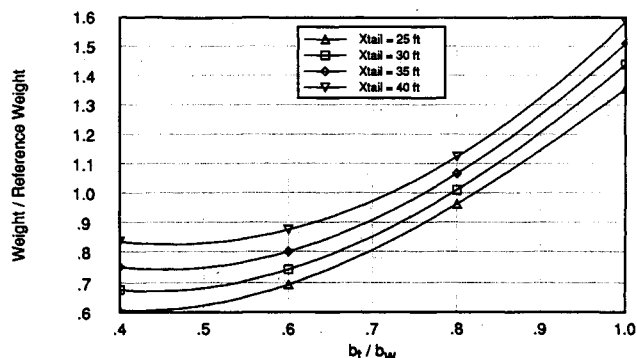

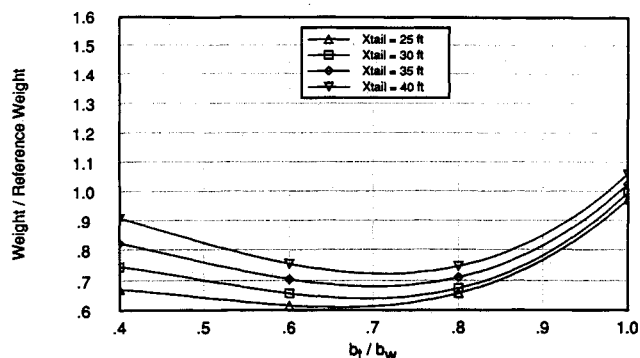Fig. 11 Relative weight vs span ratio and tail length (symmetric box, fixed span).

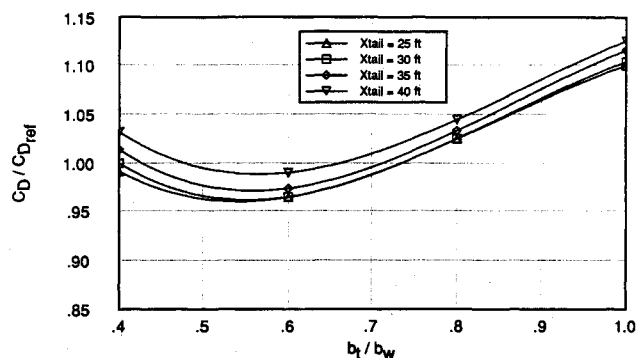Fig. 12 Relative weight vs span ratio and tail length (asymmetric box, fixed span).

Fig. 13 Relative drag vs span ratio and tail length (symmetric box, fixed weight).

contrast, suggest similarly large weight savings. Another reason is that the fixed vertical tail height has the effect of reducing the tail anhedral as the joint is moved outboard. Figure 12 shows the same results for the asymmetric-spar joined wings. It is evident that the asymmetric structure is considerably lighter. The weight penalty of the tip-joined configurations is reduced substantially by concentrating material in the corners of the structural box, lessening the impact of smaller root chord. On the other hand, the weight of the joined wings with the joint very far inboard is slightly higher. This is because the tail with the asymmetric model suffers from less spar depth to carry the bending moment from the large tail downloads. The 40% reduction in structural weight shown in Fig. 12 for $b_t/b_w = 0.7$ is in good agreement with the results of Ref. 5.

Trimmed Drag—Fixed Structural Weight

The joined-wing designs with lowest drag differ markedly from those with lowest structural weight. The optimal joined-wing design involves a compromise between achievable weight savings and drag reduction. This can be done in several ways. In this study, structural efficiency was exploited by increasing the wing span until the weight of the joined-wing design matched that of the conventional reference airplane. This span increase leads to a reduction in induced drag and a corresponding reduction in cruise drag.

Figure 13 shows the relative drag with fixed structural weight (variable span) for configurations with symmetric spars. The structural weight advantages tend to dominate, but the structural efficiency of the shortest tail arms are counteracted by increased trim drag. The values of X_{tail} used for the joined-wing cases shown here are much smaller than that of the conventional reference geometry. The impact of these short tail arms on overall mission performance will be investigated in future studies, but it should be recognized that $C_{L_{max}}$ and elevator control are reduced on these close-coupled configurations and other design constraints may tend to in-

crease the tail arm. The best joined wing with a symmetrical box structure has a tail span ratio b_t/b_w of 0.6, a span 12% larger than that of the reference case, and achieves a drag savings of approximately 3.5%.

Fixed-weight drag comparisons using the asymmetric spar model are shown in Fig. 14. A drag savings of about 11% is predicted, illustrating that the more efficient structure allows a greater wing span (18% larger than the reference wing) at fixed weight. It is also evident that the optimum joint location moves outboard to about 70% span. This is because the asymmetric spar incurs less weight penalty than the symmetric design as the joint is moved outboard, whereas outboard joints are aerodynamically beneficial. Joined wings with asymmetric spars also seem less sensitive to tail arm, with a 9% drag improvement predicted for $X_{tail} = 40$ ft.

Sensitivity to Other Design Variables

To identify the sensitivity of these results to changes in several of the other parameters, baseline values of b_t/b_w and X_{tail} were selected for the two structural representations and calculations were made with widely varying values of relative aspect ratio, wing taper, extent of the structural box in fractions of the local chord, and static margin. The span ratio and tail length were fixed for this comparison with $b_t/b_w = 0.6$ and $X_{tail} = 30$ ft. Results are shown in Fig. 15.

The effect of relative aspect ratio (hence the effect of tail area S_t/S_w) at this fixed value of b_t/b_w is small, with less than 1% change in drag. Lower tail aspect ratios start to show larger penalties, and one may conclude that joined wings should have a tail aspect ratio similar to the wing aspect ratio. Smaller tail aspects ratios (larger tail areas) may be preferred on the basis of control authority since the total tail volume of these joined-wing designs is considerably lower than the reference case. Indeed, this may be an important constraint in the use of some joined-wing configurations for certain applications.

Surprisingly, and unlike the conventional case, wing taper has almost no effect on the drag at fixed weight. This is a consequence of two competing forces. Increasing the wing taper ratio results in a smaller root chord, and, although the usual wing root bending moment M_x is smaller for a joined wing, much of the wing structural weight is still concentrated near the root to resist the M_z moment. Therefore, it would be expected that smaller root chords (larger taper ratios) would produce a structural weight penalty. This is indeed the case as the wing with a taper ratio of 0.2 has 3% greater wing span than the case with a taper ratio of 0.35, but with the same structural weight. So, although the highly tapered wing would have less induced drag, the additional wing twist required of the less tapered wing produces greater nose-up pitching moment, reducing the high tail download, and reducing the trim drag sufficiently to counteract the penalty due to its shorter span. With smaller static margins, the trim drag savings would not be expected to offset the structural penalty.

Increasing the fraction of the wing chord occupied by the structural box permits material to be distributed more appro-
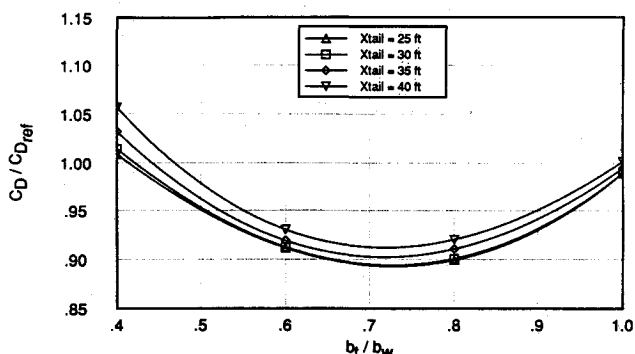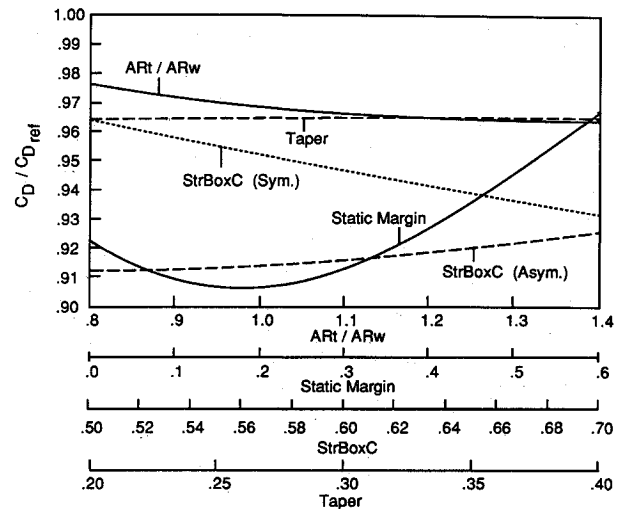

Fig. 15 Effect of design parameters on relative drag.

priately for reacting the M_z moments. It may, therefore, be desirable to extend the structural box as far forward and aft as possible, as long as the resulting loss in effective spar depth is not significant. The properties and layout of the high-lift system dictate the practical limits of this modification. The structural box of the baseline cases extended over half the chord (StrBoxC = 0.5). For the asymmetric model, the spar was located from 13 to 63% chord, and utilized 80% of the available wing thickness. Figure 15 indicates that, for the symmetric box, an additional drag savings of about 2% could be achieved if StrBoxC were increased to 0.6 with further saving available with even larger boxes. Similar analyses using the asymmetric box model have produced a somewhat different trend—results are relatively insensitive to changes in structural box chord. This is partly because the asymmetric box is better able to withstand the M_z moment components, even with small box chords. As the structural box chord is increased, the airfoil thickness at the location of the corner stringers is reduced, offsetting the potential advantages of increased box chord.

Reducing the static margin also reduces the joined-wing drag. With a static margin of 0.3 (based on the fixed reference chord) the predicted drag is 5% lower than the base case. Reducing the static margin further does not help since this moves the wing forward. (Recall that the distance from c.g. to tail root X_{tail} is fixed.) As the wing moves forward, the tail forward sweep increases, resulting in an inefficient structural arrangement. Reducing the static margin of the conventional configuration and performing the same optimization produces nearly the same drag savings at fixed weight.

Conclusions

The analysis and design method described here provides a powerful tool for evaluating the effects of several parameters on the trimmed performance of joined-wing aircraft. The rapid turnaround time permits examination of many candidate designs and promotes an understanding of fundamental design tradeoffs prior to a more application-specific design study.

The results suggest that joined wings with inboard joint locations near 60–75% of the span, with both surfaces of similar aspect ratio, are optimal for the selected design condition. The use of asymmetric material distribution in the spar is important to fully exploit the potential of the joined-wing concept, leading to a substantial reduction in cruise drag at fixed structural weight. For symmetrical spar designs, a wing layout with a greater chordwise extent of the structural box would further reduce drag at fixed weight, but this is far less important for the asymmetrical spar designs. The best lifting

Fig. 14 Relative drag vs span ratio and tail length (asymmetric box, fixed weight).

systems achieve drag reductions at fixed weight of 5% with symmetrical boxes and 11% for the asymmetric designs.

Although these calculations are not detailed sufficiently to conclude that joined wings are attractive alternatives to conventional designs, they are sufficiently promising to encourage more detailed studies. The concept seems best suited to aircraft that, because of the fuselage and engine layout, demand small tail lengths. Designs that would permit large chordwise extents of the structural box but are strongly constrained by wing t/c would also be likely candidates. Those designs for which the structural weight of the lifting system is not particularly important would be least likely to benefit from potential performance changes noted here. Particular attention in future studies should be given to the effect of the short tail lengths on $C_{L_{max}}$ and required control power and on the possibility and prevention of aft wing buckling.

References

[1]Wolkovitch, J., "The Joined Wing: An Overview, "Journal of Aircraft, Vol. 23, No. 3, 1986, pp. 161–178.

[2]Selberg, B., and Cronin, D., "Aerodynamic and Structural Optimization of Positive and Negative Stagger Joined-Wing Configurations," AIAA Paper 86-2626, Oct. 1986.

[3]Letcher, J., "V-Wings and Diamond-Ring Wings of Minimum Induced Drag," Journal of Aircraft, Vol. 9, No. 9, 1972, pp. 605–607.

[4]Samuels, M. F., "Structural Weight Comparison of a Joined and a Conventional Wing," Journal of Aircraft, Vol. 19, No. 6, 1982, pp. 485–491.

[5]Miura, H., Shyu, A., and Wolkovitch, J., "Parametric Weight Evaluation of Joined Wings by Structural Optimization," Journal of Aircraft, Vol. 25, No. 12, 1988, pp. 1142–1149.

[6]Kroo, I., LinAir—A Discrete Vortex Weissenger Method for Rapid Analysis of Lifting Surfaces, Desktop Aeronautics, Palo Alto, CA, 1987.

[7]Kroo, I., "A General Approach to Multiple Lifting Surface Design and Analysis," AIAA Paper 84-2507, Oct. 1984.

[8]O'Banion, J., Jhou, J., Stearman, R., and Smith, S., "A Study of Joint Fixativity in a Joined-Wing Aircraft," Society of Automotive Engineers, TP-871048, April 1987.

[9]Hajela, P., "Reduced Complexity Structural Modeling for Automated Airframe Synthesis," NASA CR-177440, May 1987.